

Doppler radar radial wind assimilation for the tornado outbreak on May 6, 2012

*¹Sho YOKOTA, ¹Masaru KUNII and ²Hiromu SEKO

¹Meteorological Research Institute, ²Meteorological Research Institute/JAMSTEC

1. Introduction

A strong tornado with F3 scale was generated in Tsukuba City on May 6, 2012. It moved northeastward over the Kanto Plain, and caused serious damage. Besides the Tsukuba tornado, two tornadoes were observed a few ten kilometers north of the Tsukuba tornado. Tsukuba tornado passed 15 km north of the Meteorological Research Institute (MRI), and the lower vortex associated with the tornado, as well as its precipitation areas, was well captured by the Doppler radar of the MRI. Although data assimilation of the high-resolution data, such as Radar data, is important to reproduce small-scale phenomena like tornadoes in the numerical models, it has not been performed in this case yet. In this study, Doppler wind data observed by the MRI-Radar were assimilated with an ensemble Kalman filter and the impact of the assimilation of Doppler wind data was evaluated.

2. Experimental design

In this study, a Nested Local Ensemble Transform Kalman Filter (Nested-LETKF) system was used with 12 ensemble members. Figure 1 shows the outline of the system. In Outer-LETKF, horizontal grid interval is 15 km and hourly observation data were assimilated with 6 hour intervals. In Inner-LETKF, horizontal grid interval is 1.875 km and the data obtained every 10 minutes were assimilated with 1 hour intervals. To assess the impact of the Doppler wind observations, two experiments were performed. The first one is "CTL" experiment, in which conventional observations that are used in the Japan Meteorological Agency (JMA) operational model were assimilated in both Outer- and Inner-LETKF. Another is "VR" experiment, in which the Doppler wind observed by MRI-Radar was added to the assimilation data of Inner-LETKF. The Doppler wind data used for VR were ones with the elevation angles less than 5.0 degrees and with the horizontal resolutions of about 2.5 km. Other settings of VR were the same as CTL. After the data assimilation experiments, downscaling experiments with the grid interval of 350 m were carried out in VR and CTL from the analyzed fields of 13 members (12 perturbations and one analysis) of 10:00 JST on May 6, 2012.

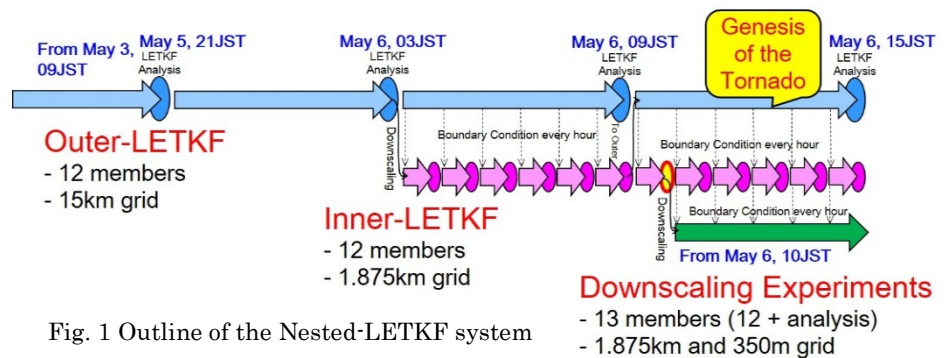


Fig. 1 Outline of the Nested-LETKF system

3. Results and correlation analysis

In the downscaling experiments, two vortices were formed in both VR and CTL. Figure 2 and 3 show the maximum velocity and the path of the southern vortex in these experiments, respectively. The path of the vortices were several kilometer north of the observed tornado in both VR and CTL. In VR, however, the southern vortex became stronger and passed about 2 km closer to the observed

tornado than those in CTL. To clarify what factors caused those differences, we focused on low level humidity at 20 m height ($Q_{v\text{-low}}$) and Storm Relative Helicity (SReH) at 10:00 JST. Figure 4 shows the difference of $Q_{v\text{-low}}$ and SReH between VR and CTL. The correlations between $Q_{v\text{-low}}$ and the maximum velocity of the vortex (V_{max}) and between SReH and the latitude where the vortex existed when it passed 140E (L140) were also calculated by coarse-grained $Q_{v\text{-low}}$ and SReH at 15 km resolution in the 13 members in VR (not shown). $Q_{v\text{-low}}$ was larger at the south of the genesis point of the vortex in VR (Fig. 4, left), and it had positive correlation with V_{max} there. Therefore, larger $Q_{v\text{-low}}$ at the south of the genesis point of the vortex made the V_{max} larger. On the other hand, SReH was larger at the north of the genesis point of the vortex in VR (Fig. 4, right), and it had negative correlation with L140 there. In addition, SReH was smaller at the south of the precipitation area in VR (Fig. 4, right), and it had positive correlation with L140 there. Therefore, increase of SReH at the north of the genesis point of the vortex and decrease of SReH at the south of the precipitation area caused that the path of the vortex shifted southward.

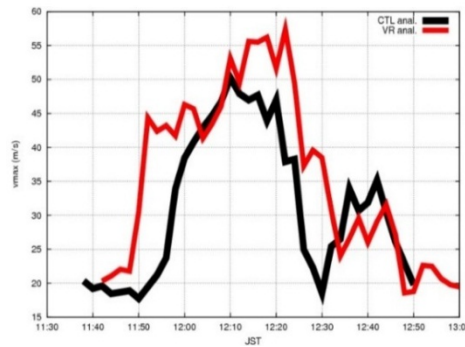


Fig. 2 The time series of maximum velocity of the south vortex at 20 m height in the downscaling experiment using analyses at 10:00 JST on May 6 as initial conditions (black: CTL, red: VR).

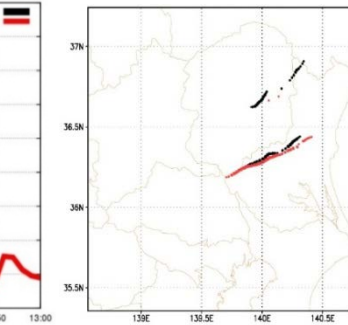


Fig. 3 The path of high relative vorticity areas at 20 m height ($> 0.03 \text{ s}^{-1}$) in the downscaling experiment using analyses at 10:00 JST on May 6 as initial conditions (black: CTL, red: VR).

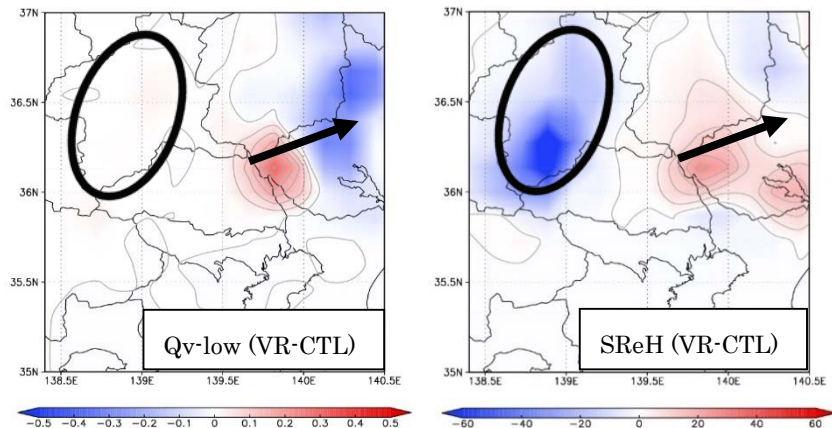


Fig.4 The difference of $Q_{v\text{-low}}$ [g kg^{-1}] (left) and SReH [$\text{m}^{-2} \text{s}^{-2}$] (right) between the analyses of VR and CTL at 10:00 JST on May 6. Contour intervals are 0.05 [g kg^{-1}] and 5 [$\text{m}^{-2} \text{s}^{-2}$], respectively, drawn only in positive. Ellipses show the precipitation region at 10:00 JST on May 6, and arrows show the path of the vortex in the downscaling experiments.

4. Summary

The vortex became stronger and the path of the vortex became closer to the reality by the assimilation of Doppler wind data observed by the MRI-Radar. The wind speed of the vortex had correlation with $Q_{v\text{-low}}$ at the south of the genesis point of vortices, and the location of the vortex had correlation with SReH at the north of the genesis point of vortices and the south of the precipitation area. Therefore, proper correction of these values by data assimilation of efficient observation data is important for better reproduction of the vortex.

Acknowledgements

The authors thank the 2nd Laboratory, Meteorological Satellite and Observation System Research Department, MRI for providing the Doppler radar data. This study was supported by "Strategic Programs for Innovative Research (SPIRE), Field 3" and "Tokyo Metropolitan Area Convection Study for Extreme Weather Resilient Cities (TOMACS)".